Proceedings of the ASME 2018 13th International Manufacturing Science and Engineering Conference
MSEC2018
June 18-22, 2018, College Station, TX, USA

MSEC2018-6406

THERMAL DESIGN AND TESTING OF A PASSIVE HELMET HEAT EXCHANGER WITH ADDITIVELY MANUFACTURED COMPONENTS

Kailyn Cage[1], Monifa Vaughn-Cooke, Mark Fuge
University of Maryland
College Park, Maryland, USA
[1]Contact Author

Briana Lucero, Dusan Spernjak, John Bernardin
Los Alamos National Laboratory
Los Alamos, New Mexico, USA

ABSTRACT

Additive manufacturing (AM) processes allow for complex geometries to be developed in a cost- and time-efficient manner in small-scale productions. The unique functionality of AM offers an ideal collaboration between specific applications of human variability and thermal management. This research investigates the intersection of AM, human variability and thermal management in the development of a military helmet heat exchanger. A primary aim of this research was to establish the effectiveness of AM components in thermal applications based on material composition. Using additively manufactured heat pipe holders, the thermal properties of a passive evaporative cooler are tested for performance capability with various heat pipes over two environmental conditions.

This study conducted a proof-of-concept design for a passive helmet heat exchanger, incorporating AM components as both the heat pipe holders and the cushioning material targeting internal head temperatures of ≤ 35ºC. Copper heat pipes from 3 manufactures with three lengths were analytically simulated and experimentally tested for their effectiveness in the helmet design. A total of 12 heat pipes were tested with 2 heat pipes per holder in a lateral configuration inside a thermal environmental chamber. Two 25-hour tests in an environmental chamber were conducted evaluating temperature (25ºC, 45ºC) and relative humidity (25%, 50%) for the six types of heat pipes and compared against the analytical models of the helmet heat exchangers.

Many of the heat pipes tested were good conduits for moving the heat from the head to the evaporative wicking material. All heat pipes had Coefficients of Performance under 3.5 when tested with the lateral system. Comparisons of the analytical and experimental models show the need for the design to incorporate a re-wetting reservoir. This work on a 2-dimensional system establishes the basis for design improvements and integration of the heat pipes and additively manufactured parts with a 3-dimensional helmet.

NOMENCLATURE

Symbol	Description	
COP	Coefficient of Performance	(dimensionless)
h_{fg}	Heat of vaporization	(J/kg)
h_{conv}	Convective heat transfer coefficient	(W/m^2 C)
h_m	Mass transfer coefficient	(m/s)
q_{cond}	Conduction flux	(W/m^2)
q_{conv}	Convection flux	(W/m^2)
q_{evap}	Evaporation flux	(W/m^2)
q_{rad}	Radiation heat flux	(W/m^2)
R_{total}	Thermal resistance of all components	(m^2 C/W)
T_{amb}, T_∞	Ambient temperature	(C)
T_{head}	Internal head temperature	(C)
T_{surf}	Surface temperature	(C)

Greek Symbol	Description	
ε_{wick}	Cloth emissivity - felt	(dimensionless)
ρ	Density	(kg/m^3)
σ	Stefan-Boltzman constant	(W/m^{2}K^4)
ϕ	Relative humidity	(%)

INTRODUCTION

We present the preliminary results from the Helmet Heat Exchanger project. The overall goals of this work are to design, build, test, and manufacture a helmet heat exchanger while incorporating components fabricated by additively manufactured processes. The heat exchanger is being developed for military applications, and specifically designed for integration with a PASGT GI helmet (Personnel Armor System for Ground Troops). The approach and finding lend themselves to other types of helmets, such as hard hats and sport helmets. This research focuses on the proof-of-concept of the integrated system with an outline for continuing work.

The novel aim of this research was to incorporate additively manufactured materials in a specific thermal application (Figure 1). Functionally, the AM parts were required to perform as both thermal heat pipe holders and padding for holding the helmet on the head, enacting human comfort. Polyurethane (PUR) material manufactured with Fused Deposition Modeling (FDM), maintained thermal comfort (<35℃), while holding the heat pipes and providing the padding leading to a secure dimensional fit. Previous research into the bulk capabilities of the material allowed for this material to be integrated into the passive thermal design.

HELMET HEAT REGULATION BACKGROUND

Helmets have been used in wars for centuries. The United States adopted the European helmet model "Hadfield" design in the development of the "M1 – Steel Pot" helmet in 1942 [1]. Since the development of the M1 helmet, the United Stated has continuously improved helmet design throughout the last 70 years. After the introduction of M1 (1942), subsequent helmet designs including the PASGT (1980), Advanced Combat Helmet ~ ACH (2005), Future Assault Shell Technology ~ FAST (2010), Enhanced Combat Helmet ~ ECH (2012), and the Helmet Electronics and Display System–Upgradeable Protection ~ HEaDS-UP (2013) were developed [1, 2]. Each generation of helmet improved on the Kevlar material called "aramid fiber" initially developed by DuPont in the 1960s [1]. The increase in military head injuries, and soldier performance highlight the critical need to address thermal performance and ergonomics through manufacturing processes and modular designs for military personnel [1, 2].

AM for Thermal Management and Human Variability

Extrusion-based AM methods such as FDM have been widely employed with various materials and biomaterials that require thermal regulation [3]. The use of AM components in flexible electronics for human interfacing applications has centralized limitations in material flexibility and thermal conductivity [3, 4]. Methods that combine AM techniques including selective laser sintering and inkjet printing, have produced 3D shape memory parts for electronics observing constant conductivities in material jetting printing processes for conductive silver ink [5]. This observation is key because it demonstrates constant conductivites in 3D printed parts. Other FDM specific applications have noted the need to explore the thermal properties including thermal conductivity of FDM printed parts [3, 4, 6, 7]. Infill density has been shown to have a significant impact on thermal and electrical conductivity in FDM printers [8]. However, the differences in thermal condutivity between parts has not been caputured. There are still many challenges with regulating thermal conductivities and thermal stability for flexible materials, although polyamides have exhibited thermal stability in FDM parts printed at temperatures under 430℃ [9]. Thermal regulation is critical in human interfacing applications because unreliable applications could lead to safety concerns for the human wearer.

Human variability plays a major role in the thermal management of the AM parts that directly interface with humans. Due to the biomechanical and anthropometric differences in human parameters, shape conforming and flexible material-based AM parts are necessary to accommodate geometric differences [4, 10]. For thermal management in human variability, thermal conductivity for AM printed parts should be standardized [9], enabling consistent thermal performance. For military helmet applications in hot, dry climates consistent thermal performance could reduce instances of heat exhaustion [11-12].

Mobile Heat Exchangers

Mobile heat exchangers provide a solution for addressing thermal comfort for military and industrial workers in various climates. Nag et al. [13] determined that a water-cooled garment with a tube-based closed loop cooling system and insulated icepack impeded the body's natural cooling process due to condensation. As an alternative to tube-based cooling, air-based cooling was evaluated and determined to be inferior to water cooling due to the low heat capacity of air and mechanical inefficiency [14]. The application of mobile heat exchangers as alternatives to both air- and water-cooled systems [13-14] has yielded promising results, while material-driven [15-16] and engine-powered [17-19] cooling systems have proven to be highly efficient in heat removal and power.

Evaporative heat transfer characteristics are important for measuring heat loss and cooling capacity in wearables with limited airflow. X. Liu and Holmer [20] demonstrated that evaporative heat dissipation is dependent on relative humidity. Knitted structure helmets provided optimal evaporative heat transfer under wind and solar conditions at 30% relative humidity (RH). The influence of wind velocity on evaporative and convection heat transfer is also supported [21], demonstrating the importance of air gaps in heat transfer. Dry heat dissipation (conduction, convection, and radiation) is significantly reduced (50% RH) in helmets while wet (evaporative) heat dissipation occurs at 68-78% RH [22], with critical effects from material thickness, material type [22], and wind velocity or passive cooling [23].

The application of phase-change material (PCM) in mobile heat exchangers plays critical role, introducing opportunities for incorporating passive approaches [24-31]. The evaluation of mobile heat exchangers that assess the efficiency of power, passive, and material-based approaches are important in design considerations for the development a thermally optimal and versatile military helmet.

Passive Thermal Regulation Approaches

Passive approaches for thermal regulation have been widely applied in bicycle helmet design. Several researchers evaluated convection heat loss, cooling power, and ventilation efficiency at head angles of 0° and 30° [32-34]. A weak correlation between exposed scalp area and heat transfer [33], suggests that the vent location may not greatly increase heat loss. Additionally, a tilted head angle of 30° with and without a visor resulted in increased

heat loss to the scale area, suggesting that visors may assist in thermal comfort maximization for convection heat loss [32, 34]. Investigations of thermal manikin heads [35-37] revealed the importance of cooling the front and rear areas of the head for improved thermal comfort [22].

Quantitative Measurement Fit for Human Head

Human-centered research is essential in safety critical scenarios for the product design process. During crash events, prevalent amounts of head injuries in children were related to the gap between the head and skull [38]. In an effort to address fit issues in helmets, Perret-Ellena et al. [39] developed the "Helmet Fit Index (HFI)" which is a tool for assessing the fit of a helmet to the human head based on anthropometry. Ellena [40] conducted a follow-up study that assessed the effectiveness of the HFI on a population of 117 subjects finding it to be a good predictor compared to subjective feedback of helmet fit from a global context (standoff distance, gap uniformity, and head protection proportion). Moreover, 3D systems were more conservative in measuring stand-off distances and provide a systematic process for assessing helmet accommodation [41]. Head length and breadth were more robust for measuring standoff distances for fit than head circumference [41], while considering hair thickness [42].

Fit for Customization

Customization in traditional manufacturing systems is expensive but designs that fail to fit the end user, in safety critical events, can lead to serious injury or death. Sizing (fit for target sample) and grading (range of sizes) methods are fit parameters that can be used for mass customization with modularity and optimization techniques. Sizing limits the number of products for a population while grading is the relationship between sizes, which is important for wearable products. Other studies have attempted to measure customized products for dynamic stability and fit, shape, and augmented personalization [44-46]. These studies emphasize identifying design parameters for customization alternatives [45].

PRELIMINARY RESULTS FOR MATERIAL SELECTION

Thermal properties, including thermal conductivities have been repeatedly mentioned in the literature as important areas for future work. In addition, flexibility, comfomence and conductivity are important for assessing the variation in fit and thermal comfort. A 1-D Conduction experiment was performed to assess the variation in thermal conductivities as a result of layer height, infill density, and material (Acrylonitrile Butadiene Styrene (ABS), Polylactic Acid (PLA), PUR), Table 1. Each material maintainted a lower thermal conductivity experimentally at small infill densities and large layer heights, Polyurethane (PUR) provided both low thermal conductivity and flexibility at 20% infill density.

The initial design of the helmet heat exchanger consists of passive cooling through evaporation. Using a PASGT GI helmet, heat pipes are paired with the additively manufactured holders/cushion to move heat from the head to the edges of the helmet. Once at the edges, the heat pipe condenser end thermally contacts a wet wicking material, covering the surface of the helmet. The wicking material is the main source of heat transfer and reservoir designs for liquid will be considered in the future.

The design and testing of the system is handled in two phases, the first proof-of-concept phase, presented herein, and consists of lateral heat pipe testing of the layers of the system. The second phase consists of lining the helmet with the AM holders and heat pipes for continued testing. In this step, heat pipe characterization will be required to consider the effects of gravity on the system performance.

Table 1 Thermal Conductivities from 1-D Conduction Experiment and Estimates at 20% Infill Density

Material	Trial	Layer Height	Thermal Conductivity (W/mC)
ABS	1	0.1	0.0430
	2	0.4	0.0601
	3	Est.	0.0560
PLA	1	0.1	0.0821
	2	0.4	0.0530
	3	Est.	0.0480
PUR	1	0.1	0.0702
	2	0.4	0.0623
	3	Est.	0.0610

Tests were conducted at Los Alamos National Laboratory, Los Alamos, New Mexico, at altitude of approximately 7400 feet, air pressure of 11.25 psi and the average near-surface air density for the site is 0.958 kg/m^3. Testing of the lateral system was performed in an environmental test chamber (Russell G-32-3), capable of controlling the internal temperatue (-30-177°C) and humidity (25-95 %RH). The system was placed inside the chamber with the condensor end of the heat pipes nearest the chamber door. The evaporator side of the heat pipes system was placed near the back end of the chamber where a radial blower drives a 1200 rpm squirrel cage blower circulating air from the bottom (inlet) to the top (outlet) of the chamber. Thus, air was blown across the wicking material, allowing for evaporative cooling.

The complete sytem consisted of a set of heat pipes, heat pipe holders, a kevlar sheet, wicking material, patch heaters, thermal insulation and thermocouples (Figure 2). The thermal insulation was placed on the floor of the chamber, with the inverted heat pipe holders and heat pipes placed against the insulation. Patch heaters were added to each heat pipe, one high temperature and low temperature patch heater. The kevlar sheet was placed over the heat pipe holders and a final wet wicking material (small Shamwow®) was laid over the kevlar, but was in contact with the evaporator end of the heat pipes. This wicking material was then placed partially in a water resevoir covered with aluminum foil to reduce excess evaporation in to the chamber.

Thermal measurements were conducted using 16 thermocouples (TCs), type-T. Two thermocouples were placed

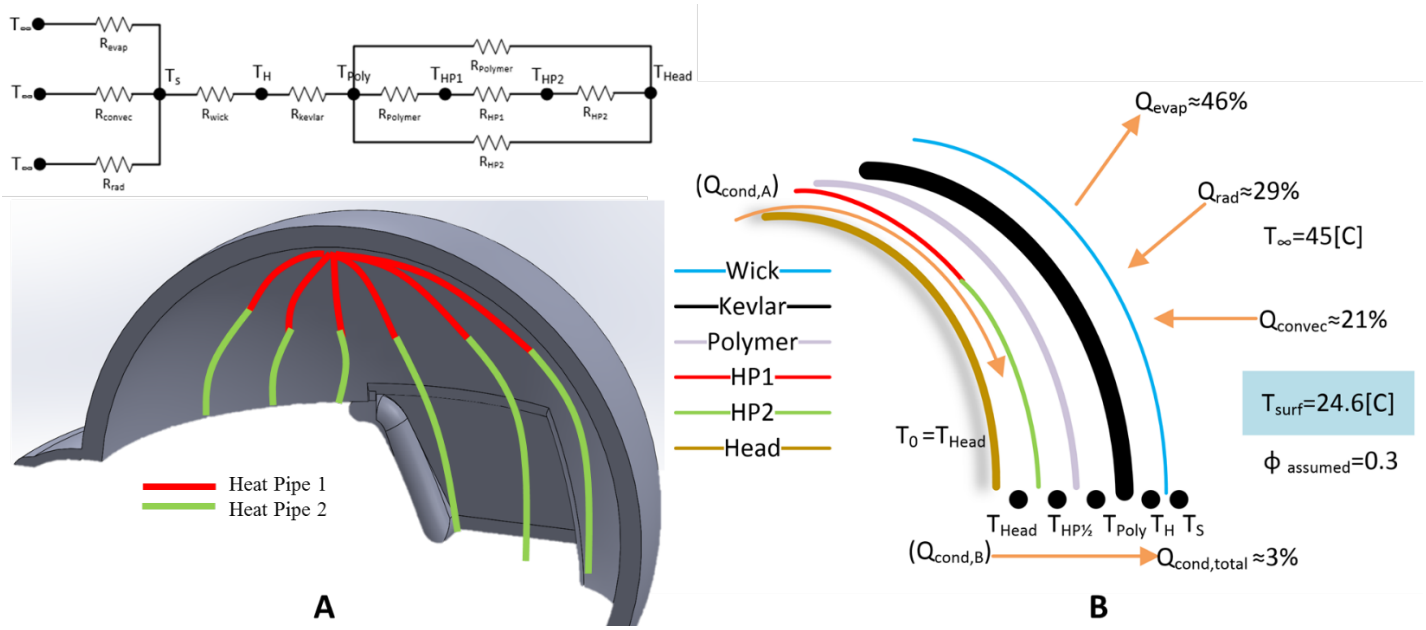

Figure 2 A) Helmet heat exchanger design and thermal resistive schematic. The helmet is covered by wicking material, touching the evaporator end of each heat pipe. Note wicking material and AM holders not shown on the CAD helmet. B) Minimal testing design point at 30% RH and an external ambient temperature of 45°C for the heat transfer mechanisms. Additional breakdown of the system shows that ~87% of the conduction occurs from passing the heat from one heat pipe to the next ($Q_{cond,A}$) while ~13% is had through the entire assembly ($Q_{cond,B}$).

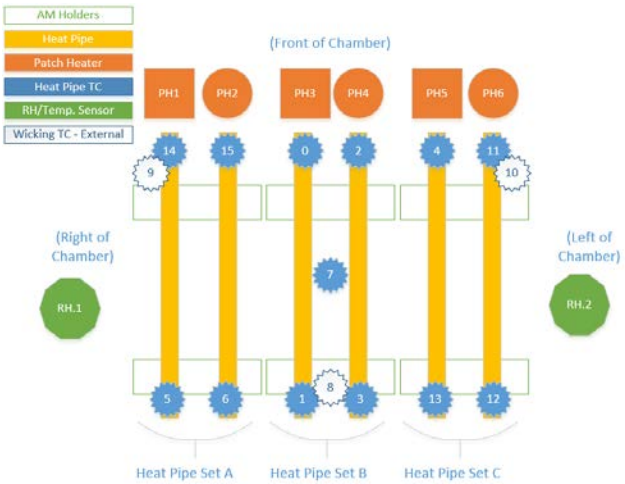

Figure 1 Experimental test schematic for environmental chamber testing of the lateral configuration. The heat pipes were covered with the Kevlar sheet and wicking material with continual wetting.

on each heat pipe, one on each end. A single TC was placed under the kevlar but above the heat pipe holders to acquire the internal temperature of the helmet (#7). Three additional TCs were placed under the wicking material, but above the the kelvar at the front and back of the kevlar sheet (#8-10). A schematic layout of the test set-up is shown in Figure 2.

Six sets of heat pipes were tested in a lateral configuration. The lateral testing (Figure 2 and Figure 3) was done as a precursor to the helmet test when the heat pipes would be bent against the lining of the helmet (Figure 1A). As such, heat pipe characterization at 0° angle was concluded and presented in this research. Curved testing is planned as a continuation of this research.

Heat pipe holders were designed in Solidworks® to securely fit the dimensions of each heat pipe holder set with a small gap between the top surface of the holder and heat pipe. The holders were printed from a Lulzbot TAZ 5 printer, which is an FDM process categorized under the material extrusion AM process. The heat pipe holders were produced at 60m/s print speed, 0.4mm layer height, 20% infill density, and grid fill pattern. All other settings remained at the factory settings in Cura

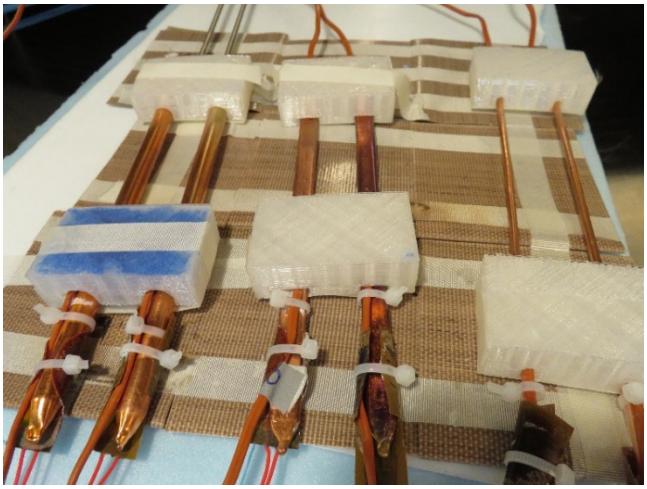

Figure 3 Heat pipe sets with 3D printed holder mates with the heat patches on the front end, TCs on both ends, and insulation under the entire set-up.

(a 3D printer slicing application). These AM settings produced parts with greater material conformance and heat transfer efficiency, Table 1. Two heat pipes of the same dimensions were assigned to a one heat pipe holder set where one holder was attached at the top portion of the heat pipes and the other was attached to the bottom portion, Figure 3.

Testing of the system consisted of 15-minute ramping times and 6-hour dwell times at each target temperature and relative humidity. The temperatures were varied from 25-45°C with relative humidity controlled at 25% and 50%. The experimental test matrix can be found in Table 2. During the test, the relative humidity was held constant while the temperature was varied for each of the two humidity sets. Therefore, each test consisted of two "sets" of tests with two different temperatures and two different RH values.

The temperature and relative humidity of the ambient conditions were recorded with two Omega OM-EL-USB-PLUS2 relative humidity/temperature sensors. Both sensors were placed on the floor of the chamber, on either side of the system set-up. The sensors were centered along the length of the system to get the data, sampling twice a minute.

Six sets of heat pipes were tested in two separate batch runs. Each 25-hour test was run with three sets of pipes, with the AM holders setting pipe sets A and B together, but not touching. The 12 heat pipes tested are remunerated in Table 3

ANALYTICAL THERMAL PERFORMANCE MODELS

Theoretical modelling of the system was performed for two different models of various complexity. The first model included a Newton-Raphson root-finding method to solve for the transcendental, non-linear energy balance as a proof-of-concept model, containing high-level assumptions. The second was a more detailed, Engineering Equations Solver (EES) model calling all thermodynamic properties from the EES tables. Both analytical models were developed with the intent of comparing against the experimental data. The two models both solved for the surface temperature of the Shamwow® covering the Kevlar as an energy balance of the cooling effects. Of note, the contact resistance between the wicking material and the Kevlar shell has been included in the wet cloth resistance of the wicking material.

Assumptions for calculating the energy balance of the system include:

- Steady-state conditions with dry air modeled as ideal gas
- Constant properties, except for variable specific volume in temperature range of interest
- The wicking material surface is small in comparison to the large, isothermal surroundings for radiation exchange
- No heat loss/gain occurs from any surface other than the wicking material; all other helmet surfaces are considered adiabatic
- Internal convection can be neglected
- Contact resistance between wicking and cooling surface is included in the resistance of the wicking material
- All heat transfer occurs along the length of the heat pipes; there is no conduction from one heat pipe set to another
- The internal temperature of the helmet is set at the human comfort temperature of 35°C

Table 2 Thermal testing design matrix for testing at two different temperatures and relative humidities.

Set	Segment	Type	Step Time (min)	Temp. (°C)	Humidity (%RH)
1	1	Ramp	15	45	25
	2	Dwell	360	45	25
	3	Ramp	15	25	25
	4	Dwell	360	25	25
2	5	Ramp	15	45	50
	6	Dwell	360	45	50
	7	Ramp	15	25	50
	8	Dwell	360	25	50

Table 3 Heat pipe description with DAQ channel and patch heater assignment.

ID	Manufacturer	Length (mm)	Diameter (mm)	Heat Pipe
HP1	Enertron	200	8	A
HP2	Enertron	200	8	B
HP3	Wakefield-Vette	200	8.4	A
HP4	Wakefield-Vette	200	8.4	B
HP5	Thermocool	250	3	A
HP6	Thermocool	250	3	B
HP7	Enertron	150	8	A
HP8	Enertron	150	8	B
HP9	Wakefield-Vette	150	8.4	A
HP10	Wakefield-Vette	150	8.4	B
HP11	Thermocool	150	4	A
HP12	Thermocool	150	4	B

For the sake of model simplicity, the radial conduction and the internal convection of the helmet was neglected. There are two modes of conduction, (1) conduction along the length of the heat pipes, originating from the center of the head and transmitting outward toward the edge of the helmet through two sets of heat pipes ($Q_{cond,A}$) and (2) conduction through the layers of the system outward ($Q_{cond,B}$). Conductive heat transfer from one set of heat pipes to another axially was neglected in these models and will be addressed in future work [47].

Using a surface energy balance of the wicking material, the equations (1)-(6) were implemented. The convection, conduction, gain and radiation are all additive heat flux terms. The evaporation is the only term that provides cooling to the human head and therefore to the entire helmet. The conduction is active through the metal heat pipes in contact with the wicking material and the Shamwow®. The radiation and convection (both free and forced) fluxes act on the upper surface of the Shamwow®. Equation 6 is transcendental primarily because of the nonlinearities associated with the radiation term (Equation 3) and the variable specific volume of the saturated vapor at the Shamwow® upper surface.

$$q_{cond} = \frac{T_{head} - T_s}{R_{total}} \quad (1)$$

$$q_{conv} = h_{conv} \cdot \left(T_\infty - T_{surf}\right) \quad (2)$$

$$q_{rad} = \sigma \cdot \varepsilon_{wick} \cdot \left({T_\infty}^4 - {T_{surf}}^4\right) \quad (3)$$

$$q_{evap} = h_m \cdot h_{fg \cdot water \cdot s} \cdot (\rho_{water \cdot s} - \phi_{assumed} \cdot \rho_{water \cdot \infty}) \quad (4)$$

$$q_{cond} + q_{rad} + q_{conv} = q_{evap} \quad (5)$$

$$COP = \frac{T_{surf}}{T_{head} - T_{surf}} \quad (6)$$

The Coefficient to Performance for each of the heat pipes was calculated from Equations 1-6, where T_∞ is the ambient temperature, T_{surf} is the Shamwow® external surface temperature, and T_{head} is the head temperature. The surface temperatures were calculated using both the EES and Newton-Raphson methods and plugged into the equation for system effectiveness. The ambient temperatures and relative humidities were gathered from the USB data logger.

Experimental Results Analysis

Testing of the lateral system was performed as outlined in the previous sections. Initial desires to test at humidity closer to 10% R.H. was thwarted by the fiberglass insulation of the system and achievable ambient temperatures. The minimum ambient temperature allowed at the 10% RH is 42°C, so the original D.O.E. was maintained at 25% RH.

The results of the experimental data were gathered in 25-hour increments, spanning the two temperatures and relative humidities, Figure 6. The data was analyzed in individual relative humidity or temperature tests independent of the other recorded sets. The internal head temperature was based upon the condenser temperatures of the various heat pipes. Overall there was a positive temperature gradient from the ambient to the human head, meaning there was some cooling occurring. However, there were several cases, primarily at the higher temperatures and relative humidity, where there was a negative gradient (internal temperature was greater than the ambient).

Since the two control variables (temperature and relative humidity) were tested at two different levels, an Analysis of Variance (ANOVA) was used to evaluate the data collected during testing [48-49]. This analysis tool allows for the evaluation of the variance within the data based on the independent variable (ambient temperature and humidity) levels and measures their significance. From this equation, the numerical variation in the data can be compared to the controlled variation of the temperature and relative humidity variables (Figure 4 and Figure 5) allowing for experimental validation [50]. For this paper, the data was analyzed at a 90% percent confidence interval. To perform the analysis, the ambient data values (Table 2) were averaged and graphed.

The COP of heat pipes in the entire lateral configuration can be seen in Table 4 for only the B set of pipes. The second heat pipe of each set, set A, provided similar behavior so their COPs were not reported. Surprisingly, 4 of the 6 heat pipes had the best COP at the higher humidity, and lower temperature (25ºC, 50%R.H.). At the lowest relative humidity tested and the lowest temperature, only heat pipe #4 showed a better COP, while HP#2 showed the best COP at the lower humidity and higher temperature.

Investigation into the cause of the higher temperature performance lead to graphing of the individual heat pipes for both the A/B sets. However, for the sake of brevity, only B was included in this publication (Figure 6). Investigation into the experimental set-up leading to the higher temperature COPs, determined several causes: (1) The ambient chamber RH, while set was not constant over the course of each dwell and (2) the evaporator contact with the wicking material was not always consistent. The chamber on the high temperatures, necessitated the use of the humidity control with ranges between 28 and 50% R.H. Accordingly, the higher temperatures might have influenced the performance of the heat pipes. And finally, the wicking material was wrapped under the Kevlar and placed in contact with the evaporator end of each set of heat pipes. During the test set-up no quality control mechanism was in place to ensure all sets received the same contact area. Test set 2 (HP 8, 10, & 12) would be a prime example of both these faults. Thus, the anticipated results of the best COP at lower temperatures was not achieved.

When all the heat pipes are compared for their performance, the best heat pipe for this specific application would be HP12 (Thermocool 4mm DIA x 150mm length). The two other 150mm length heat pipes had larger diameters (~8mm DIA) and performed considerably worse at both ambient temperatures. This trend of the larger diameter pipes to not be as effective, hold true for the 200mm length as well. The smallest diameter and longest heat pipe (HP 6) had the second-best performance for both temperatures. Thus, the performance of the heat pipes is more diameter limited, than length limited.

This spread of the COP for all heat pipes, while showing decent performance, does not account for the requirement of maintaining the internal temperature at 35ºC. In all but 5 of the six cases, the measured internal head temperature at the optimal COP, was within this bound. The HP#2 was 1.4 ºC over the limit and when compared against the performance of the A set (HP#1), this heat pipe fails to meet this requirement entirely. The other heat pipes of Set B, show similar behavior for Set A and thus cannot be discounted in the final design. This leads the designers to believe the best options for thermal performance is limited to diameters less than 4mm and length no greater than 200mm.

While these tests were run at 0° inclination, the heat pipes are all operating at the greatest effectiveness. Once the heat pipes are placed in the PAGST helmet and bent to the contours of the helmet, the effectiveness is expected to decrease. The design already accounts for having two heat pipes in series (see Figure 1A), which can handle the counter-flow issues of bending to the helmet shape. As this future testing will demonstrate, heat pipe combinations of various lengths and diameters will be considered.

Analytical Results

At the minimal design point of 30% R.H. and an external ambient temperature of 45°C, the heat transfer

breakdown was determined to be primarily lead by evaporation as shown in Figure 1B. The conduction is primarily lead by the transfer of one heat pipe to the next laterally ($Q_{cond,A}$) at ~87% while the conduction through the helmet shows a transfer of ~13% ($Q_{cond,B}$) for the sum total of 3% of the overall heat transfer. Radiative and convective losses were secondary and tertiary, respectively, in the systems heat transfer.

A comparison of the surface temperatures (Ts) from the two set of calculations can be seen in Figure 4 and Figure 5 with the average condenser temperature (Thead) of 35°C. At the 45ºC temperature (Figure 5), the EES calculations are undershooting the actual performance while the Newton Raphson calculations overshoot the performance. And at the 25ºC temperature, both calculations sets undershoot the predicted values. The differences may be partially attributed to the temperature dependent property capabilities of the EES calculations in comparison to the manual Excel calculations. Within the Excel calculations only the specific volume of the saturated vapor for the saturated air at the edge of the boundary layer was calculated as a function of Shamwow® surface temperature, T_{surf}. All other thermo-physical properties were assumed constant.

Given that experimental testing only occurred at 25 and 50% RH, the results cannot be used to express the entire range of relative humidities of operation. But understanding the limitation of evaporative cooling with the wet-bulb temperatures guided the decision to test at the 50% R.H. as the maximum. Once saturation of the surrounding air is reached, no cooling will occur and heating of the human head could be an issue. From the models, this heating potential has a greater possibility of happening at the higher temperatures with lower humidities.

The results of the models and the data bring to light the operating limitations of current model. Even at the lateral configuration, where maximum heat pipe performance is anticipated, the system cannot sufficiently cool at relative humidities over 30% and above ambient temperatures of 45°C. At ambient conditions of 25°C, the helmet heat exchanger can operate up to humidities near 50% R.H. As the initial application was to be used in military environments with less than 40% R.H., and higher temperatures (in excess of 45°C), additional cooling mechanisms may need to be considered in the helmet integration.

FUTURE WORK

This work was preliminary design efforts to integrate additively manufactured materials into a helmet heat exchanger as the heat pipe holders and the helmet/human interface. Initial modeling and simulation work shows that there is merit to the design of the AM holders as the material properties of the printed Ninja Flex PUR, had sufficient thermal conductivity of 0.19 W/m-K [51]. This thermal insulation allowed for heat to be transported along the heat pipes axially (Qcond, A), and not be lost radially through the holders and the helmet (Qcond, B). However, additional research to develop a 'composite structure' with flexible AM material impregnated with a heat-conductive material is planned, that will line the contours of the helmet.

With this proof-of-concept completed in these initial steps, the following is planned to complete this study in the future: (1) Final holder design & manufacture, including interface mounts, (2) Holder material strength tests and final thermal characterization, (3) Heat pipe characterization in final Holder/Helmet configuration including comparison of individual HP characterization to lateral effectiveness and gravity effects, and (4) Completion of human variability testing with helmet fit to test subjects.

CONCLUSION

The efforts of this research were to design, test and develop a helmet heat exchanger with additively manufactured parts capable of accounting for human variability. A passive evaporative cooler design with heat pipes and 3D printed holder/cushioning was proposed. Using NinjaFlex material and thin heat pipes, the human head would move head along the inside of the helmet to the wicking material where evaporation would cool the system. The holders could be placed systematically for human comfort and sizing depending on the final heat pipe selection.

Table 4 Heat pipe COP for all the B heat pipes with the best COP highlighted. The A set of heat pipes acted like these B set, and was not reported.

HP2 – Enertron (8mm DIA x 200mm)					
% Amb. R.H.	$T_{ambient}$ (°C)	$T_{surface}$ (°C)	T_{head} (°C)	%R.H.	COP
25.0	24.0	16.0	23.4	39	2.2
	30.0	24.7	36.4	30	2.1
50.0	24.0	22.3	27.1	50	4.6
	42.0	29.6	37.7	47	3.7
HP4 – Wakefield-Vette (8.4mm DIA, flat x 200mm)					
% Amb. R.H.	$T_{ambient}$ (°C)	$T_{surface}$ (°C)	T_{head} (°C)	%R.H.	COP
25.0	24.0	18.7	27.8	39	2.1
	30.0	30.5	41.8	30	2.7
50.0	24.0	22.3	29.6	50	3.1
	42.0	32.5	42.6	47	3.2
HP6 – Thermocool (3mm DIA x 250mm)					
% Amb. R.H.	$T_{ambient}$ (°C)	$T_{surface}$ (°C)	T_{head} (°C)	%R.H.	COP
25.0	24.0	21.4	27.0	39	3.9
	30.0	36.3	40.3	30	9.0
50.0	24.0	22.4	29.1	50	3.4
	42.0	35.3	41.3	47	5.9
HP8 – Enertron (8mm DIA x 150mm)					
% Amb. R.H.	$T_{ambient}$ (°C)	$T_{surface}$ (°C)	T_{head} (°C)	%R.H.	COP
25.0	24.0	23.1	26.4	40	7.0
	42.5	23.4	34.5	25	2.1
50.0	24.0	19.1	29.6	50	1.8
	42.0	25.5	35.8	28	2.5
HP10 - Wakefield-Vette (8.4mm DIA, flat x 150mm)					
% Amb. R.H.	$T_{ambient}$ (°C)	$T_{surface}$ (°C)	T_{head} (°C)	%R.H.	COP
25.0	24.0	25.1	27.3	40	11.8
	42.5	27.2	34.5	25	3.7
50.0	24.0	21.6	32.4	50	2.0
	42.0	28.9	34.8	28	4.9
HP12 – Thermocool (4mm DIA x 150mm)					
% Amb. R.H.	$T_{ambient}$ (°C)	$T_{surface}$ (°C)	T_{head} (°C)	%R.H.	COP
30.00	24.00	27.16	28.56	40.00	19.42
	42.50	30.91	36.18	25.00	5.87
50.00	24.00	24.08	32.71	50.00	2.79
	42.00	32.42	36.83	28.10	7.35

Initial design requirements were leveraged on the design for performance and integration. Analytical models using

EES and Newton-Raphson root-finiding methods were employed to identify the feasibility of the design. Assumptions and simplifiations begot optimistic results at temperatures below 45°C and humidities less than 50% R.H. The analytical results were compared against experimental results for a lateral system with no curvature. This prelimanry work provides positive results with the current design, and has identified areas of additional improvement and testing.

ACKNOWLEDGMENTS

We acknowledge the AAPP Program at LANL for funding this project. We express our gratitude to all AET-1 personnel for their dedicated assistance throughout this work. This work is referenced by LA-UR-17-20959.

REFERENCES

[1] Council, N. R. (2014). Review of Department of Defense test protocols for combat helmets. Washington, D.C.: National Academies Press.

[2] Owens, B. D., Kragh Jr, J. F., Wenke, J. C., Macaitis, J., Wade, C. E., & Holcomb, J. B. (2008). Combat wounds in operation Iraqi Freedom and operation Enduring Freedom. *Jo. of Trauma and Acute Care Surgery*, 64(2), 295-299.

[3] M. Vaezi, S. Chianrabutra, B. Mellor, and S. Yang, (2013) "Multiple material additive manufacturing – Part 1: a review," *Virt. and Physical Prototyping*, vol. 8, pp. 19-50.

[4] H. Yang, W. R. Leow, and X. Chen,(2018) "3D Printing of Flexible Electronic Devices," *Small Methods, 2(1)*

[5] M. Zarek, M. Layani, I. Cooperstein, E. Sachyani, D. Cohn, and S. Magdassi, (2016). "3D Printing of Shape Memory Polymers for Flexible Electronic Devices," *Advanced Materials*, vol. 28, pp. 4449-4454.

[6] Dev, A., Hansen, C.J., Courter, B., Bi, J. and Savane, V., (2017). Mechanical Testing of FDM Parts for Process Simulation. *Proc.of NAFEMS Wld. Cong.* (p. 11-14).

[7] Courter,B., Savane,V., Bi,J., Dev,S. and Hansen,C.J., (2017). Finite Element Simulation of the Fused Deposition Modelling Process. *Proc. of NAFEMS Wld Cong.* (p.11-14).

[8] R. Singh, G. S. Sandhu, R. Penna, and I. Farina, (2017) "Investigations for Thermal and Electrical Conductivity of ABS-Graphene Blended Prototypes." *Materials, 10*(8), 881.

[9] T. Rahim, A. Abdullah, H. M. Akil, D. Mohamad, and Z. Rajion, (2017), "The improvement of mechanical and thermal properties of polyamide 12 3D printed parts by fused deposition modelling," *Exp. Poly. Ltrs.* 11.

[10] Bogerd, C.P., J.M. Aerts, S. Annaheim, P. Bröde, G.de Bruyne, A.D. Flouris, K. Kuklane, T. Sotto-Mayor and R. M. Rossi.(2015). "A review on ergonomics of headgear: Thermal effects." *Int. Jo. Ind. Ergs. 45(Supp. C)*: 1-12.

[11] Stacey, M., D. Woods, D. Ross and D. Wilson (2014). "Heat illness in military populations: asking the right questions for research." *Jo. Royal Army Med. Corps* **160**(2): 121-124.

[12] Nunneley, S. A. and M. J. Reardon (2002). "Prevention of heat illness." *Med. Asp. Of Har. Envir.,* **1**: 209-230.

[13] Nag, P., Pradhan, C., Nag, A., Ashtekar, S., & Desai, H. (1998). Efficacy of a water-cooled garment for auxiliary body cooling in heat. *Ergs., 41*(2), 179-187.

[14] Epstein, Y., Shapiro, Y., & Brill, S. (1986). Comparison between different auxiliary cooling devices in a severe hot/dry climate. *Ergs., 29*(1), 41-48.

[15] Pourmohamadian, N., Philpott, M. L., & Shannon, M. A. (2004). Connection Methods for Non-Metallic, Flexible, Thin, Microchannel Heat Exchangers: Air Conditioning and Refrigeration Center. College of Engineering. University of Illinois at Urbana-Champaign.

[16] Zhang, G., Zhang, X., Huang, H., Wang, J., Li, Q., Chen, L.-Q., & Wang, Q. (2016). Toward Wearable Cooling Devices: Highly Flexible Electrocaloric Ba0.67Sr0.33TiO3 Nanowire Arrays. *Advanced Materials*, 28(24), 4811-4816.

[17] Elbel, S., Bowers, C. D., Zhao, H., Park, S., & Hrnjak, P. S. (2012). Development of Microclimate Cooling Systems for Increased Thermal Comfort of Individuals. *Inter. Refrig. and Air Cond. Conf.,* 2149-2157.

[18] Ernst, T. C., & Garimella, S. (2009). Wearable engine-driven vapor-compression cooling system for elevated ambients. *Jo. of Therm. Sci. and Eng. App.s, 1*(2), 025001.

[19] Ernst, T. C., & Garimella, S. (2013). Demonstration of a wearable cooling system for elevated ambient temperature duty personnel. *App. Therm. Eng., 60*(1), 316-324.

[20] Liu, X., & Holmér, I. (1995). Evaporative heat transfer characteristics of industrial safety helmets. *App. Ergs. 26*(2), 135-140.

[21] Sun, Y., & Jasper, W. J. (2015). Numerical modeling of heat and moisture transfer in a wearable convective cooling system for human comfort. *Build. & Envir., 93, Part 2*, 50-62.

[22] Pang, T. Y., Subic, A., & Takla, M. (2014). Evaluation of thermal and evaporative resistances in cricket helmets using a sweating manikin. *App. Ergs., 45*(2), 300-307.

[23] Brühwiler, P. A. (2003). Heated, perspiring manikin headform for the measurement of headgear ventilation characteristics. *Meas. Sci. & Tech., 14*(2), 217.

[24] Kalaiselvama, S., Kumara, K. S., & Sriramb, V. (2016). Study of Heat Transfer and Pressure Drop Characteristics of Air Heat Exchanger Using PCM for Free Cooling Applications. *Therm. Sci.*, 20(5), 1543-54.

[25] Chelliah, A., Karthick, B., Vimalkodeeswaran, A., & Hariram, V. (2015). Helmet Cooling System Using Phase Change Material for Long Drive. *Jo. of Eng. and App. Sci., 10(4),* 1770-1773.

[26] Sezgin, Y. C., & Celik, M. (2015). PCM-cap to provide thermal comfort for human head. *Ext. Phys. & Med., 4*(Suppl 1), A81-A81.

[27] Vigneswaran, G., & Arulmurugan, L. (2014). Improving Thermal Comfort in Industrial Safety Helmet Using Phase Change Material. *Inter. Jo. of Sci. Eng. and Tech Research, 3*, 0712-0715.

[28] Jovanovic, D. B., Karkalić, R., Tomić, L., Veličković, Z., & Radaković, S. (2014). Efficacy of a novel phase change

material for microclimate body cooling. *Therm. Sci., 18*, 657-665.
[29] Fok, S. C., Tan, F. L., & Sua, C. C. (2011). Experimental investigations on the cooling of a motorcycle helmet with phase change material. *Therm. Sci., 15*(3).
[30] Ge, H., & Liu, J. (2013). Keeping Smartphones Cool with Gallium Phase Change Material. *Jo. H. Tran. 135*(5), 054.
[31] Shen, W., & Tan, F.-L. (2010). Thermal management of mobile devices. *Therm. Sci, 14*, 115-124.
[32] Bruhwiler, P.A., Buyan, M., Huber, R., Bogerd, C.P., Sznitman, J., Graf, S.F., & Rosgen, T. (2006). Heat transfer variations of bicycle helmets. *Jo. of Sports Sci., 24*(9), 999-1011.
[33] Brühwiler, P. A., Ducas, C., Huber, R., & Bishop, P. A. (2004). Bicycle helmet ventilation and comfort angle dependence. *European Jo.of App. Phys., 92*(6), 698-701.
[34] Martínez, N., Psikuta, A., Rossi, R. M., Corberán, J. M., & Annaheim, S. (2016). Global and local heat transfer analysis for bicycle helmets using thermal head manikins. *Int. Jo. of Ind. Ergs., 53*, 157-166.
[35] De Bruyne, G., Aerts, J.-M., Vander Sloten, J., Goffin, J., Verpoest, I., & Berckmans, D. (2012). Quantification of local ventilation efficiency under bicycle helmets. *Int. Jo. of Ind. Ergs., 42*(3), 278-286.
[36] Chaplin, D. V., (2010) "Thermoelectric crash helmet cooling system with no mechanically moving components or fluids." U.S. Patent 12,459,991.
[37] Rivara, F. P., Astley, S. J., Clarren, S. K., Thompson, D. C., & Thompson, R. S. (1999). Fit of bicycle safety helmets and risk of head injuries in children. *Injury Prevention, 5(3)*, 194-197.
[38] Perret-Ellena, T., Subic, A., Pang, T. Y., & Mustafa, H. (2014). The helmet fit index-A method for the computational analysis of fit between human head shapes and bicycle helmets. *Paper presented at icSPORTS 2014*.
[39] Ellena, T., Subic, A., Mustafa, H., & Pang, T. Y. (2016). The Helmet Fit Index – An intelligent tool for fit assessment and design customization. *App. Ergs., 55*, 194-207.
[40] Meunier, P., Tack, D., Ricci, A., Bossi, L., & Harry, A. (2000). Helmet accommodation analysis using 3D laser scanning. *App. Ergs., 31*(4), 361-369.
[41] Perret-Ellena, T., Skals, S. L., Subic, A., Mustafa, H., & Pang, T. Y. (2015). Anthropometric Investigation of Head and Face Characteristics of Australian Cyclists. *Procedia Engineering, 112*, 98-103.
[42] Luximon, A., Zhang, Y., Luximon, Y., & Xiao, M. (2012). Sizing and grading for wearable products. *Computer-Aided Design, 44*(1), 77-84.
[43] Huang, S.-H., Yang, Y.-I., & Chu, C.-H. (2012). Human-centric design personalization of 3D glasses frame in markerless augmented reality. *Adv. Eng. Info. 26*(1), 35-45.
[44] Liu, B. S. (2008). Incorporating anthropometry into design of ear-related products. *App. Ergs., 39*(1), 115-121.
[45] Pang, T.Y., Babalija,J., Perret-Ellena,T., Lo, T.S.T., Mustafa, H., & Subic,A.(2015). User Centered Design Customization of Bicycle Helmets Liner for Improved Dynamic Stability and Fit. *Proc. Engineering, 112*, 85-91
[46] S. Pheasant, (1996), Bodyspace: anthropometry, ergonomics, and the design of work, 2nd ed. London; Bristol, PA: Taylor & Francis.
[47] Incropera, F., D.P. Dewitt, T.L. Bergman and A.S. Levine. (2007). Fundamentals of Heat and Mass Transfer. John Wiley & Sons, Inc.
[48] Frigon, N., and D. Matthews. (1997). Practical Guide to Experimental Design. John Wiley & Sons, Inc.
[49] Montgomery, D.C. (1997). Design and Analysis of Experiments. John Wiley & Sons, Inc.
[50] Otto, K. and K. Wood. (2001). Product Design: techniques in Reverse Engineering and New Product Development. Prentice Hall, Inc.
[51] Lasance, C. (2001). The Thermal Conductivity of Rubbers &Elastomers.https://www.electronicscooling.com/2001/11/the-thermal-conductivity-of-rubbers-elastomers

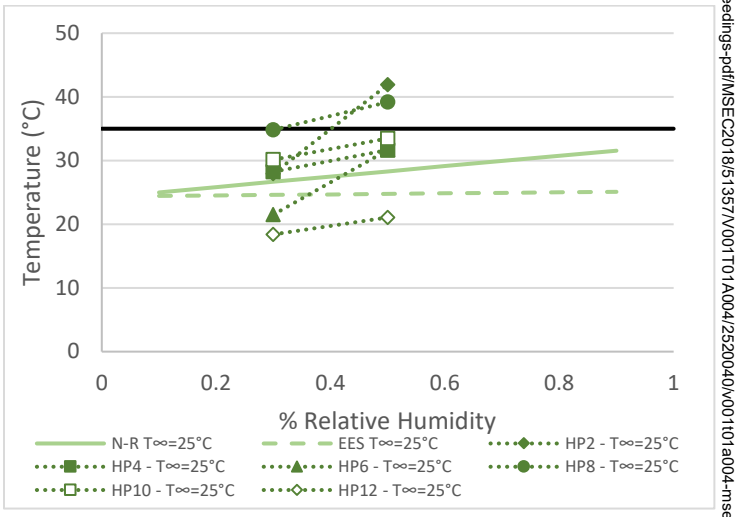

Figure 4 Model comparison: Analytical models vs. the two experimental tests at 25°C for all B heat pipes.

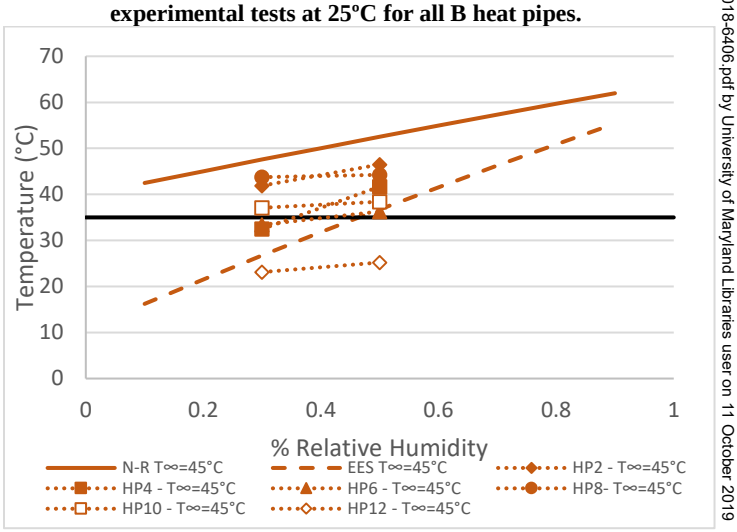

Figure 5 Model comparison: Analytical models vs. the two experimental tests at 45°C for all B heat pipes.

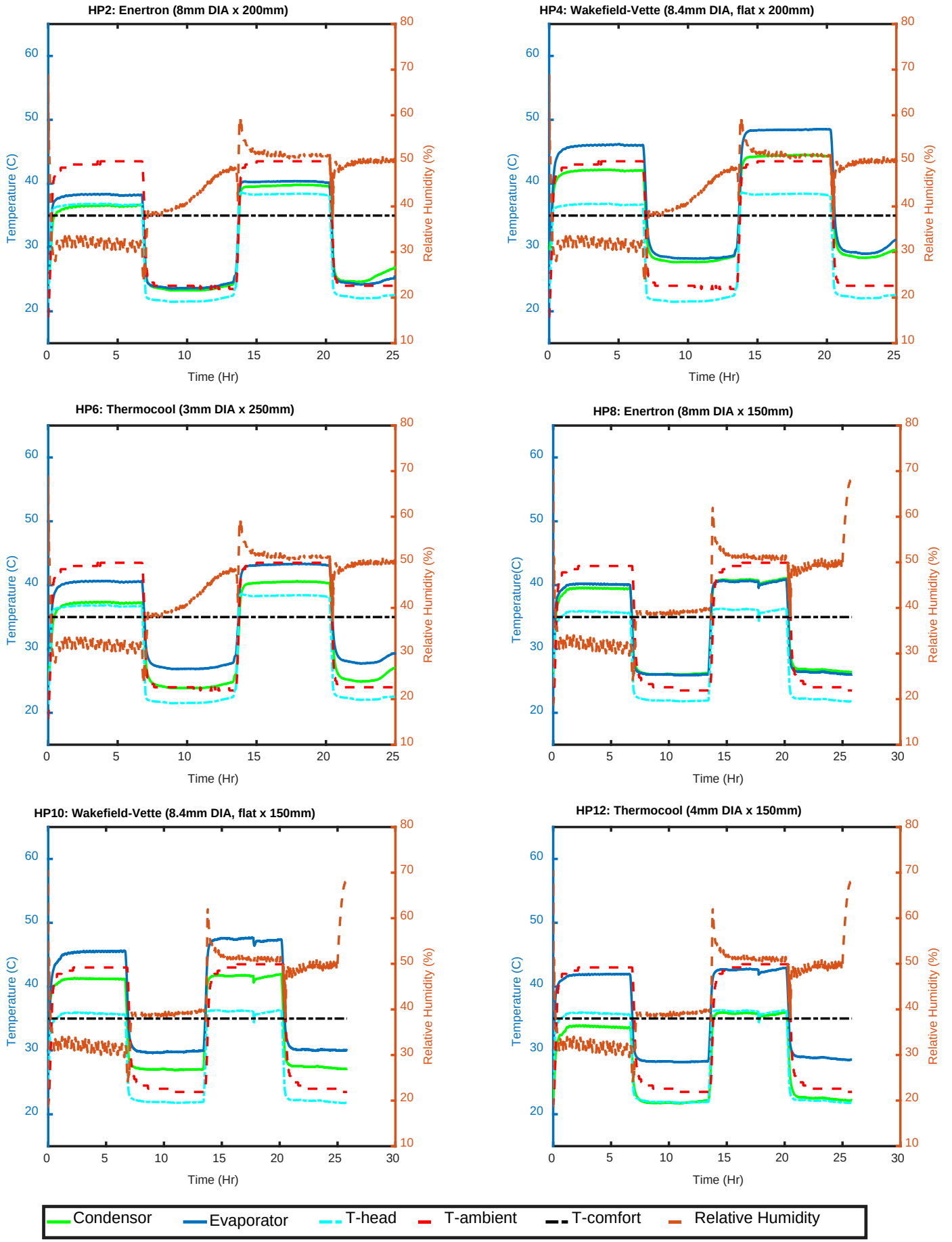

Figure 6 Individual heat pipe performance comparing head temperature, relative humidity, human comfort temperature and ambient temperatures conditions for all the B pipes of Table 3.